Science of the Total Environment 576 (2017) 210–224

Contents lists available at ScienceDirect

Science of the Total Environment

journal homepage: www.elsevier.com/locate/scitotenv

Air quality across a European hotspot: Spatial gradients, seasonality, diurnal cycles and trends in the Veneto region, NE Italy

Mauro Masiol [a,b,*], Stefania Squizzato [a,c], Gianni Formenton [d], Roy M. Harrison [b,1], Claudio Agostinelli [e]

[a] Center for Air Resources Engineering and Science, Clarkson University, Box 5708, Potsdam, NY 13699-5708, USA
[b] Division of Environmental Health and Risk Management, School of Geography, Earth and Environmental Sciences, University of Birmingham, Edgbaston, Birmingham B15 2TT, United Kingdom
[c] Dipartimento Scienze Ambientali, Informatica e Statistica, Università Ca' Foscari Venezia, Campus Scientifico via Torino 155, 30170 Venezia, Italy
[d] Dipartimento Regionale Laboratori, Agenzia Regionale per la Prevenzione e Protezione Ambientale del Veneto, Via Lissa 6, 30174 Mestre, Italy
[e] Dipartimento di Matematica, Università degli Studi di Trento, via Sommarive 14, Povo, Trento, Italy

HIGHLIGHTS

- CO, NO_x, O_3, SO_2, PM_{10}, $PM_{2.5}$ were hourly measured at 43 sites from 2008 to 2014.
- Interannual trends, seasonal and daily cycles were investigated and quantified.
- Site classification has been evaluated using data-depth analysis.
- Trends in measured concentrations were coupled with emission inventories.
- Despite significant drops in levels, NO_x and PM are still critical pollutants.

GRAPHICAL ABSTRACT

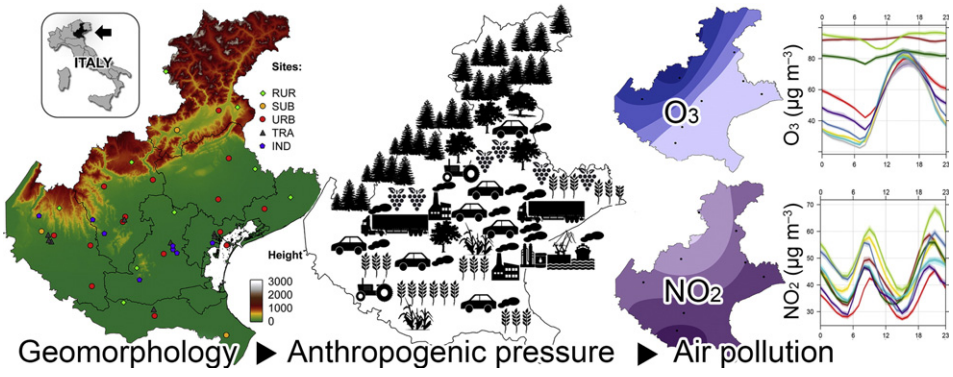

ARTICLE INFO

Article history:
Received 30 August 2016
Received in revised form 5 October 2016
Accepted 6 October 2016
Available online 24 October 2016

Editor: D. Barcelo

Keywords:
Air pollution
Nitrogen oxides
Particulate matter
Veneto
Trends

ABSTRACT

The Veneto region (NE Italy) lies in the eastern part of the Po Valley, a European hotspot for air pollution. Data for key air pollutants (CO, NO, NO_2, O_3, SO_2, PM_{10} and $PM_{2.5}$) measured over 7 years (2008/2014) across 43 sites in Veneto were processed to characterise their spatial and temporal patterns and assess the air quality. Nitrogen oxides, PM and ozone are critical pollutants frequently breaching the EC limit and target values. Intersite analysis demonstrates a widespread pollution across the region and shows that primary pollutants (nitrogen oxides, CO, PM) are significantly higher in cities and over the flat lands due to higher anthropogenic pressures. The spatial variation of air pollutants at rural sites was then mapped to depict the gradient of background pollution: nitrogen oxides are higher in the plain area due to the presence of strong diffuse anthropogenic sources, while ozone increases toward the mountains probably due to the higher levels of biogenic ozone-precursors and low NO emissions which are not sufficient to titrate out the photochemical O_3. Data-depth classification analysis revealed a poor categorization among urban, traffic and industrial sites: weather and urban planning factors may cause a general homogeneity of air pollution within cities driving this poor classification. Seasonal and diurnal cycles were investigated: the effect of primary sources in populated areas is evident throughout the region and drives similar patterns for most pollutants: road traffic appears the predominant potential source shaping the daily

* Corresponding author at: Center for Air Resources Engineering and Science, Clarkson University, Box 5708, Potsdam, NY 13699-5708, USA.
E-mail address: mauro.masiol@gmail.com (M. Masiol).
[1] Also at: Department of Environmental Sciences/Center of Excellence in Environmental Studies, King Abdulaziz University, PO Box 80203, Jeddah, 21589, Saudi Arabia.

http://dx.doi.org/10.1016/j.scitotenv.2016.10.042

cycles. Trend analysis of experimental data reveals a general decrease of air pollution across the region, which agrees well with changes assessed by emission inventories. This study provides key information on air quality across NE Italy and highlights future research needs and possible developments of the regional monitoring network.

1. Introduction

Since the mid-90s, the European Community has adopted increasingly stringent standards for abating emissions and for improving the air quality. The main steps in the legislative process were the Framework Directive 96/62/EC, its subsequent daughter Directives and the more recent Directive 2008/50/EC. As a consequence, a general improvement of air quality has been recorded in the last decade. However, current and future EU standards are still breached in some European regions, the so-called hotspots, e.g., Northern Italy, Benelux and some Eastern Countries (Putaud et al., 2004, 2010). Under this scenario, the development of additional successful strategies for emission mitigation and the implementation of measures for air quality control are two major questions addressed by policy makers and in scientific research, respectively.

Following the implementation of the EC Directives, local and national authorities are required to monitor air quality. Measurement data are primarily managed by local agencies to assess the extent of air pollution, check if standards are complied with, and, in case of the exceeding of Limit Values or even lower assessment thresholds, to inform the population about potential health impacts. Beyond their original regulatory purpose, such data also represent a valuable resource: if historical data are available, long-term trends can be investigated to obtain real feedback upon the successes and failures of past and current mitigation strategies.

The Po Valley (N Italy) is neither a city nor an administrative unit, but it can be considered a megacity (Zhu et al., 2012). Currently, it is one of the few remaining and most worrying European hotspots: high levels of hazardous pollutants are commonly recorded over a wide area (~$48 \cdot 10^3$ km^2) hosting ~16 million inhabitants. The anthropogenic pressure and some peculiar geomorphological features (a wide floodplain is enclosed by the Alps and Apennine mountains) lead to frequently breaches of limit and target values imposed by EU Directives (EEA, 2016) for nitrogen oxides, ozone and particulate matter (PM).

The Veneto region (Fig. 1) is located in the eastern part of the Po Valley and extends over ~$18.4 \cdot 10^3$ km^2 ranging from high mountain environments (29% of the territory), to intermediate hill zones (15%), large and flat plain areas (56%) and ~95 km-long coastlines. From an administrative point of view, it is subdivided in 7 Provinces: Belluno (BL), Treviso (TV), Vicenza (VI), Venice (VE), Padova (PD) and Rovigo (RO). Heavy anthropogenic pressures are present almost continuously: a total of ~$4.9 \cdot 10^6$ inhabitants are resident in some large cities (>$2 \cdot 10^5$ inhabitants: Verona, Padova and Venice-Mestre) and in a number of minor towns and villages which form a continuum "sprinkled" network of urban settlements. Consequently, emissions from road traffic and domestic heating are spread throughout the region. Some industrial areas are also present, mainly close to the main cities and with distinctive features and different plant types. In addition, the Veneto lies in a strategic location linking Central, Eastern Europe and continental Italy: a dense network of international E-roads and transport hubs attract large amounts of road and intermodal traffic, mostly heavy duty diesel-powered trucks. A large percentage of the region includes agricultural fields, mostly located in the plain (intensive farming) and hilly areas (vineyards, orchards), while rural environments are present mainly in hilly and mountain regions. A land use map is provided in Fig. 1: this composite landscape inevitably makes the emission scenario of the region extremely complex and its spatial variations quite unpredictable.

This study aims to examine and describe the spatial variations, temporal trends and seasonality of air quality across the Veneto region over 7 years (2008–2014). Datasets used in this study include the mass concentration of key air pollutants as required by European air quality standards: nitrogen oxides ($NO + NO_2 = NO_x$), ozone (O_3), carbon monoxide (CO), sulphur dioxide (SO_2) and PM with aerodynamic diameter <10 μm (PM_{10}) and <2.5 μm ($PM_{2.5}$). Air quality data were measured by ARPAV (Veneto Environmental Protection Agency) through a well-established network of 43 sampling stations (ARPAV, 2014) covering a large portion of the territory (Fig. 1). A series of chemometric procedures are used to assess the extent of air pollution, to verify the effectiveness of site categorization and to find patterns commonly recorded across the Veneto or identify sites with anomalous pollution levels. The gradients of concentrations are depicted and seasonal/diurnal/weekly patterns are investigated. The long-term trends are

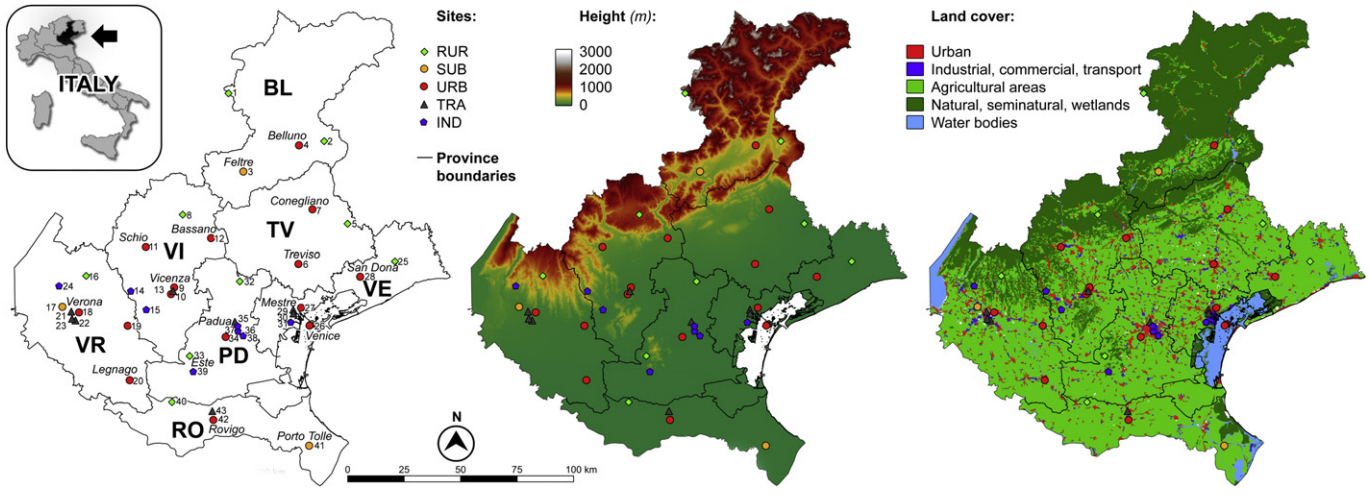

Fig. 1. Map of the Veneto region: administrative (left); terrain relief (centre); land use and cover from CORINE Land Cover 2006 data (right). Sampling sites are also represented as diamonds (RUR sites), dots (SUB and URB sites), triangles (TRA sites) and pentagons (IND sites).

seasonally decomposed and then processed to find the general orientations and drifts in air pollution over sites with a different categorization. Furthermore, long-term trends are coupled with changes in the emission inventories to verify if estimated emissions match with experimentally recorded levels of key air pollutants across the region.

2. Materials and methods

2.1. Sampling sites

The map of sites is shown in Fig. 1, while Table 1 summarises their general characteristics and measured pollutants. Fig. 1 also shows the political, relief and land use maps. Sites are identified by the initials for the province and their category. Sites were selected to fulfil some specifications: (i) data availability must cover at least four years in 2008/14; (ii) sites must be representative of most important pollution climate scenarios, such as citywide pollution, regional background or traffic and industrial hotspots and (iii) sites must be representative of differing environments (mountain, hilly, plain, coastal areas). In particular:

- At least one site was selected as rural background (RUR sites) for each Province (total 9 sites), i.e. in areas not directly influenced by trafficked roads and/or urban and industrial settlements. In particular, BL.RUR and VI.RUR are located in remote locations at high altitudes. RUR sites are fundamental to assess the background gradients at the regional scale;
- Eighteen sites were categorized as suburban (SUB) and urban (URB), i.e. broadly representative of citywide levels of air pollutants;
- A total of 8 sites were selected as representative of traffic hotspots (TRA) and placed at kerbside locations in cities experiencing heavy traffic and/or frequent road congestion events;
- Eight sites were set as representative of main industrial (IND) areas. Each site has peculiar characteristics. VE.IND is located downwind of Porto Marghera, one of the main industrial zones in Italy extending over ~12 km^2 and including a large number of different installations (thermoelectric power plants burning coal, gas and refuse derived fuels, a large shipbuilding industry, an oil-refinery, municipal solid waste incinerators and many other chemical, metallurgical and glass plants). VI.IND1 and VI.IND2 are representative of small and medium-sized tannery industries, PD.IND1 and PD.IND2 are set in an area potentially affected by a municipal solid waste incinerator plant, PD.IND3 was selected to monitor the fall-out from a steel mill and VR.IND and PD.IND4 are representative of emissions from cement plants.

2.2. Experimental

All selected sites are equipped with fully automatic analysers set to collect data on hourly (gaseous pollutants) or hourly/bihourly bases

Table 1
Characteristics of the sampling sites and analysed pollutants. Municipality refers to the territorial district where the sampling site is located: if the site is not located in the main town of a municipality, the city/town is given in brackets.

Province	No.	Code	Lat.	Long.	Height (m)	Municipality (city/town)	Site full name	Area type	Monitored pollutants
BL	1	BL.RUR1	46.339	11.802	2020	Falcade	Passo Valles	Rural background	NO_x, O_3
	2	BL.RUR2	46.163	12.361	615	Pieve d'Alpago	Pieve d'Alpago	Rural background	NO_x, O_3, SO_2, PM_{10}
	3	BL.SUB	46.031	11.906	263	Feltre	Area Feltrina	Suburban	CO, NO_x, O_3, SO_2, PM_{10}
	4	BL.URB	46.144	12.219	401	Belluno	BL-città	Urban background	CO, NO_x, O_3, SO_2, PM_{10}
TV	5	TV.RUR	45.837	12.51	14	Treviso (Mansuè)	Mansuè	Rural background	CO, NO_x, O_3, PM_{10}
	6	TV.URB1	45.672	12.238	15	Treviso	TV-Via Lancieri	Urban background	CO, NO_x, O_3, SO_2, PM_{10}, $PM_{2.5}$
	7	TV.URB2	45.89	12.307	72	Conegliano	Conegliano	Urban background	CO, NO_x, O_3, SO_2, PM_{10}
VI	8	VI.RUR	45.849	11.569	1366	Asiago	Asiago-Cima Ekar	Rural background	NO_x, O_3
	9	VI.URB4	45.759	11.736	114	Bassano	Bassano del Grappa	Urban background	NO_x, O_3 PM_{10}
	10	VI.URB1	45.56	11.539	36	Vicenza	VI-Quartiere Italia	Urban background	CO, NO_x, O_3
	11	VI.URB2	45.532	11.522	33	Vicenza	VI-Ferrovieri	Urban background	CO, NO_x, O_3, SO_2
	12	VI.URB3	45.714	11.368	190	Schio	Schio-via Vecellio	Urban background	NO_x, O_3, PM_{10}, $PM_{2.5}$
	13	VI.TRA	45.545	11.533	35	Vicenza	VI-San Felice	Urban-traffic	CO, NO_x SO_2, PM_{10}
	14	VI.IND1	45.536	11.294	154	Chiampo	Chiampo	Urban-industrial	NO_x
	15	VI.IND2	45.465	11.386	61	Montebello Vicentino	Montebello Vicentino	Suburban-industrial	NO_x
VR	16	VR.RUR	45.589	11.037	824	Boscochiesanuova	Boscochiesanuova	Rural background	CO, NO_x, O_3, SO_2, PM_{10}
	17	VR.SUB	45.462	10.911	91	Verona (Cason del Chievo)	VR-Cason	Suburban	CO, NO_x, O_3, SO_2, PM_{10}, $PM_{2.5}$
	18	VR.URB1	45.443	11.007	64	Verona	VR-Piazza Bernardi	Urban background	CO, NO_x
	19	VR.URB2	45.399	11.285	30	Verona (San Bonifacio)	San Bonifacio	Urban background	CO, NO_x, O_3, SO_2, PM_{10}, $PM_{2.5}$
	20	VR.URB3	45.183	11.311	25	Legnago	Legnago	Urban background	NO_x, O_3, PM_{10}
	21	VR.TRA1	45.444	10.963	62	Verona	VR-Borgo Milano	Urban-traffic	CO, NO_x SO_2, PM_{10}
	22	VR.TRA2	45.41	10.989	60	Verona	VR-San Giacomo	Urban-traffic	CO, NO_x SO_2
	23	VR.TRA3	45.416	10.969	65	Verona	VR-ZAI	Urban-traffic	CO, NO_x, O_3, SO_2
	24	VR.IND	45.543	10.886	183	Fumane	Fumane	Industrial	NO_x SO_2, PM_{10}
VE	25	VE.RUR	45.694	12.786	5	Concordia Sagittaria	Concordia Sagittaria	Rural background	NO_x, O_3
	26	VE.URB1	45.428	12.313	1	Venezia	VE-Sacca Fisola	Urban background	NO_x, O_3, SO_2, PM_{10}
	27	VE.URB2	45.5	12.261	1	Venezia (Mestre)	VE-Parco Bissuola	Urban background	CO, NO_x, O_3, SO_2, PM_{10}
	28	VE.URB3	45.629	12.59	3	San Donà di Piave	San Donà di Piave	Urban background	CO, NO_x, O_3, PM_{10}, $PM_{2.5}$
	29	VE.TRA1	45.49	12.218	2	Venezia (Mestre)	VE-Via Tagliamento	Urban-traffic	CO, NO_x SO_2, PM_{10}
	30	VE.TRA2	45.474	12.22	2	Venezia (Marghera)	VE-Via Beccaria	Urban-traffic	CO, NO_x, PM_{10}
	31	VE.IND	45.438	12.205	2	Venezia (Marghera)	VE-Malcontenta	Industrial	CO, NO_x SO_2
PD	32	PD.RUR1	45.594	11.909	24	Santa Giustina in Colle	S. Giustina in Colle	Rural background	CO, NO_x, O_3
	33	PD.RUR2	45.289	11.642	18	Padova (Cinto Euganeo)	Parco Colli Euganei	Rural background	NO_x, O_3, SO_2, PM_{10}
	34	PD.URB	45.371	11.841	13	Padova	PD-Mandria	Urban background	CO, NO_x, O_3, SO_2, PM_{10}
	35	PD.TRA	45.433	11.89	11	Padova	PD-Arcella	Urban-traffic	CO, NO_x, O_3, SO_2, PM_{10}
	36	PD.IND1	45.395	11.909	10	Padova	PD-APS-1-Ignoto	Urban-industrial	CO, NO_x, O_3, SO_2, PM_{10}, $PM_{2.5}$
	37	PD.IND2	45.415	11.907	10	Padova	PD-APS-2-Carli	Urban-industrial	CO, NO_x, O_3, SO_2, PM_{10}, $PM_{2.5}$
	38	PD.IND3	45.378	11.94	8	Padova	PD-Granze	Urban-industrial	PM_{10}
	39	PD.IND4	45.227	11.666	12	Este	Este	Suburban-industrial	CO, NO_x, O_3, SO_2, PM_{10}
RO	40	RO.RUR	45.103	11.554	8	Badia Polesine	Polesine-Villafora	Rural background	CO, NO_x, O_3, SO_2
	41	RO.SUB	44.95	12.333	1	Porto Tolle	Porto Tolle	Suburban	NO_x, SO_2, PM_{10}, $PM_{2.5}$
	42	RO.URB	45.039	11.79	3	Rovigo	RO-Borsea	Urban background	CO, NO_x, O_3, SO_2
	43	RO.TRA	45.074	11.782	7	Rovigo	RO-Centro	Urban-traffic	CO, NO_x, O_3, SO_2, PM_{10}

(PM_{10} and $PM_{2.5}$). QA/QC of measurements is guaranteed by ARPAV internal protocols, which fully comply with the standards required by EC Directives in-force: EN 14626:2012 for CO, EN 14211:2012 for NO, NO_2, and NO_x, EN 14212:2012 for SO_2, EN 14625:2012 for O_3. CO, NO_x, O_3 and SO_2 instruments were calibrated every day. Hourly- or bihourly-resolved PM_{10} and $PM_{2.5}$ were measured with beta gauge monitors: validation experiments were routinely conducted between gravimetric (EN 14907:2005) and automatic methods; several tests were also performed routinely (at least 1 test every week) to keep a constant check on the beta gauge samplers. Pairs of filters were measured with both methods and the results were checked to ensure that they are within the variation margins imposed by the technical protocols adopted in UNI EN 12341:2001. Some sites were not equipped with hourly PM monitors (Table 1), but may provide daily gravimetric-measured PM_{10} levels. In this case, PM was collected by low-volume samplers on filters and the mass concentration was measured by gravimetric determination (EN 14907:2005) at constant temperature (20 ± 5 °C) and relative humidity (RH, 50 ± 5%). Consequently, no diurnal patterns are investigated in such sites, but only interannual and seasonal trends.

2.3. QA/QC and data handling

Data have been validated by ARPAV through a well consolidated internal protocol (ARPAV, 2014) and according to the European standards. The full dataset was therefore used for exploratory statistics. However, the aim of this study is to detect the general behaviour of air pollution and some clearly identified high pollution episodes which occurred in 2008/14 across the region. Examples are the burning of a thousand folk fires on the eve of Epiphany (Masiol et al., 2014a) or fireworks for Christmas and other local celebrations. Consequently, preliminary data handling and clean-up are carried out to check the datasets for robustness, outliers and anomalous records. For this purpose, data greater than the 99th percentile were included for exploratory analysis but not in the trend estimation. Data were also adjusted to account for the shift in anthropogenic emissions due to the changes between local time (UTC + 1) and daylight savings time (DST). This latter correction helps in investigating daily patterns of anthropogenic emission sources.

Data were analysed using R (R Core Team, 2016) and a series of supplementary packages, including 'openair' (Carslaw and Ropkins, 2012; Carslaw, 2015), 'PMCMR' (Pohlert, 2015) and 'localdepth' (Agostinelli and Romanazzi, 2011, 2013).

2.4. Data depth classification analysis

A classification analysis was used to check the accuracy of the site categorization, i.e., to verify whether the sampling sites in a category (RUR, SUB + URB, TRA, IND) are characterised by a general homogeneity in air pollutant levels. This task is accomplished by applying a new classification technique based on statistical data depth (DD). This technique is well reviewed elsewhere (Mosler and Polyakova, 2012 and the reference therein) and recently was extended to functional and multivariate data (Ramsay and Silverman, 2006; Lopez-Pintado and Romo, 2009; Lopez-Pintado and Romo, 2011; Claeskens et al., 2014; Cuevas, 2014).

The depth of a point relative to a given dataset measures how deep the point lies in the data cloud, i.e. it measures the centrality of a point with respect to an empirical distribution (Mosler and Polyakova, 2012). DD provides an order to the observations and the rank system provided by DD can be used to perform unsupervised and supervised classification analysis. A statistical depth function should be invariant to all (non-singular) affine transformations; it reaches the maximum value at the centre of symmetry for symmetric distribution and it becomes negligible when the norm of the point tends to infinity. Another important property is ray-monotonicity, i.e. the statistical depth does not increase along any ray from the centre (Liu, 1990; Zuo and Serfling, 2000). The classical notion of data depth has been extended to functional data and the different available implementations aim to describe the degree of centrality of curves with respect to an underlying probability distribution or a sample. Some advisable properties of functional depths are the (semi-) continuity, the consistency, and the invariance under some class of transformations, which tends to vanish when the norm of a curve tends to infinity (Mosler and Polyakova, 2012).

A classification analysis was performed by using the DD-plot tool and a functional multivariate simplicial depth. First, a (empirical) simplicial depth of a *point* y with respect to a *set of points* $x = (x_1, \ldots, x_n)$ in the Euclidean space of dimension p is introduced. $S_i = S(x_{i1}, x_{i2}, \ldots, x_{ip}, x_{ip+1})$ represents the simplex obtained using $p + 1$ points in the sample. A simplex of $p + 1$ points in a space of dimension p is the convex hull of those points. Then $d(y; x_n)$ is the fraction of simplicials S_n contains y overall combinations of the $p + 1$ indices $i_1, i_2, \ldots, i_p, i_{p+1}$ in the set $1, \ldots, n$. This is a consistent estimator of the simplicial depth, which is the probability that a random simplex $S(x_1, x_2, \ldots, x_p, x_{p+1})$ will cover the *point* y when $x_1, x_2, \ldots, x_p, x_{p+1}$ are identical and independent copies of the random variable x from where the sample is drawn.

Thus, we can consider a set of (multivariate) curves $x_j(t)$, $(j = 1, \ldots, J)$ measured at time $t_1, t_2, \ldots, t_N$, i.e. $x_j(t_j)$ is a point in the Euclidean space of dimension p. In our context, $x_j(t)$ is the multivariate time series at location j (sampling site) for a set of p pollutants concentration measured at time t. Following Claeskens et al. (2014), we defined the depth of a given curve $y(t)$ according to the sample $x = (x_1(t), \ldots, x_J(t))$, denoted $d(y(t), x)$ as the weighted average of the empirical simplicial depth evaluated at any given time $t_1, t_2, \ldots, t_N$. The weights proportional to the fraction of available observations at each time is then set. This is important to be considered for the presence of missing values.

The classification is performed using the depth-versus-depth plot (DD-plot) (Li et al., 2012; Cuevas, 2014). Considering two groups of curves $x = (x_1(t), \ldots, x_J(t))$ and $z = (z_1(t), \ldots, z_K(t))$, the goal is to classify a curve $y(t)$ in one of these. Hence, we evaluate $d(y(t),x)$ and $d(y(t),z)$ that represents the depth of $y(t)$ according to x and to z. We assign $y(t)$ to the first group if $d(y(t),x) > d(y(t),z)$ and to the second group otherwise. In particular, two groups of curves will be well separated if $d(x_j(t),x) > d(x_j(t),z)$ for each observation x_j and $d(z_k(t),x) < d(z_k(t),z)$ for each observation z_k. Finally, we can plot on a Cartesian axis the points $(d(x_j(t),x),\ d(x_j(t),z))$, $j = 1, \ldots, J$ and the points $(d(z_k(t),x),d(z_k(t),z))$, $k = 1, \ldots, K$, i.e. the DD-plot. Curves (sampling sites) well classified in the first group will be plotted at the right bottom corner of the graphics, whereas curves well classified in the second group will appear at the left upper corner. Curves equally well classified in both groups will lie around the bisector line of the plot.

In this study, four site categories are used to group the sites: rural (RUR), urban and sub-urban (URB), traffic (TRA) and industrial (IND). For each couple of categories, the DD-plots are evaluated on the basis of distributions of one or more pollutants.

3. Results

A summary of data distributions during the whole study period (all available data) is provided as boxplots in Fig. 2 and maps in Fig. SI1. Concentrations are expressed as mass concentration; NO_x is expressed as NO_2, as required by EU standards. Moreover, Table SI2 reports annual average concentration and exceedances for NO_2, O_3, PM_{10} and $PM_{2.5}$. CO and SO_2 are not included because no exceedances were observed.

3.1. Carbon monoxide and sulphur dioxide

In Veneto, CO and SO_2 are not critical pollutants. CO values are well below the EC limit value and WHO guidelines (WHO, 2000), i.e. 10 mg m^{-3} as daily maximum over 8 h. The highest hourly average levels of CO over six years were recorded at VR.URB1, PD.IND2, VR.TRA3, PD.URB, VE.TRA1 and PD.IND1 (all ~0.6 mg m^{-3}); remaining sites showed concentrations between 0.2 and 0.6 mg m^{-3}.

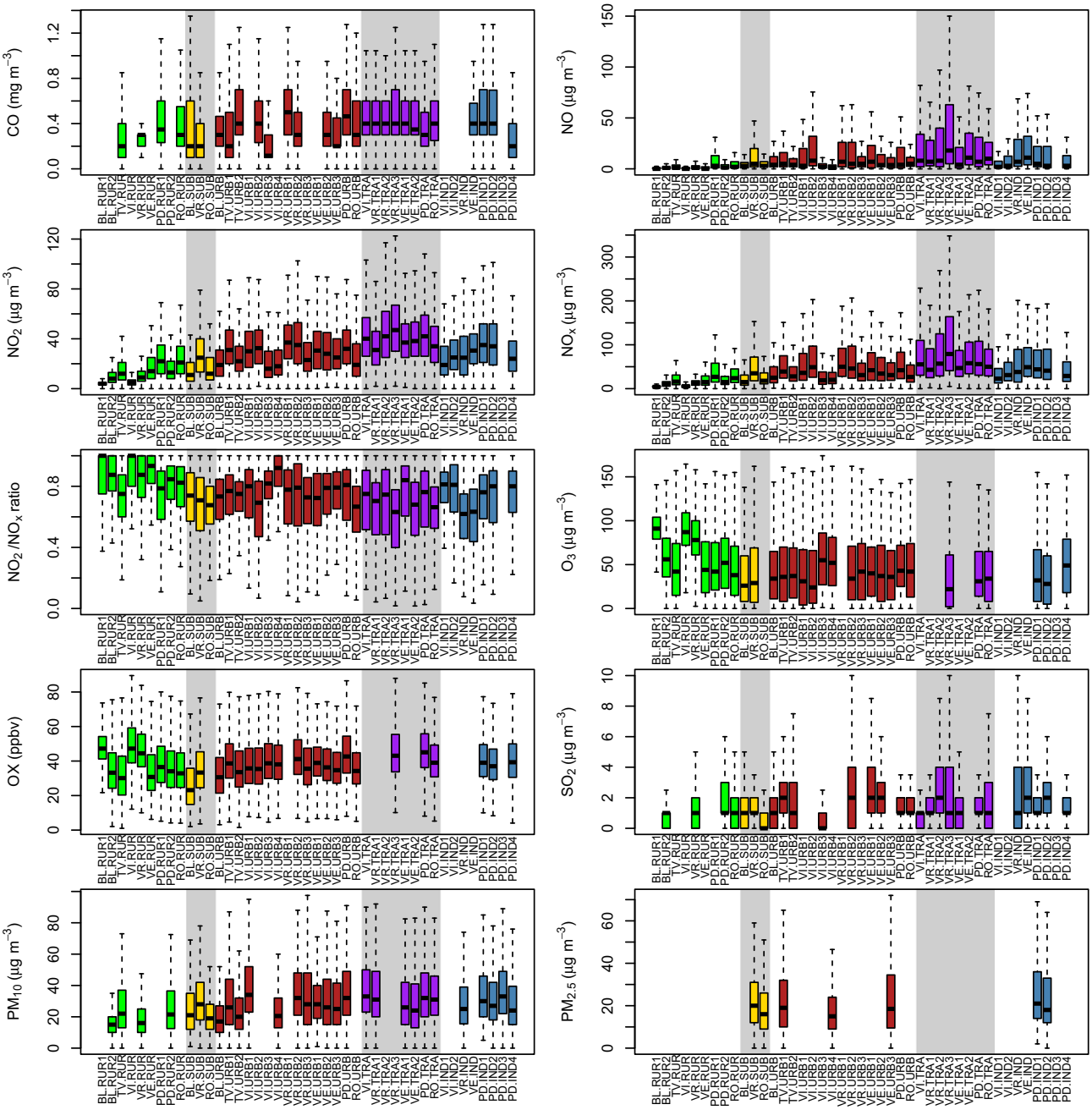

Fig. 2. Average and ranges of concentrations of the analysed pollutants as boxplots of raw data (line = median, box = inter-quartile range, whiskers = ±1.5*inter-quartile range). Sites are clustered following their categorization.

SO_2 does not show exceedances of European standards both for hourly averages (350 µg m^{-3}) and for 24-h averages (125 µg m^{-3}). The 2008/14 average concentrations across Veneto were very low, ranging from ~0.6 µg m^{-3} (often below instrumental detection limits) at VI·URB3 and RO·SUB to ~4 µg m^{-3} at some sites near Venice (VE.IND, VE.URB1). The higher levels in Venice sites can be likely associated to harbour and industrial emissions (i.e. thermal power plant, oil refinery and municipal solid waste incinerator). While the contribution of the harbour to the levels of SO_2 in Venice is still debated (Contini et al., 2015), the role of industrial emissions is well supported by the emission inventories. In 2005, about 76% of overall SO_2 emissions in the Veneto were released in the Province of Venice, of which 69% (19,742 Mg y^{-1}) came from combustion in energy and transformation industries (ARPAV, 2011).

3.2. Nitrogen oxides

When considering the short-term metrics, NO_2 does not represent a special risk for human health in Veneto: the 1-hour alert threshold of 400 µg m^{-3} was never breached, while the 1-hour average of 200 µg m^{-3} not to be exceeded more than 18 times over a calendar year was exceeded only at VR.TRA3 in 2008. However, NO_x becomes pollutants of concern when looking at the long-term metrics. The minimum average levels were found at two rural sites located in high mountain environments, while maxima were measured at a traffic site in Verona located very close to a logistic intermodal freight transport hub spanning over 4 km^2 and moving 26 million tons of goods annually (VR.TRA3). The average concentrations of NO varied from 0.5–0.6 µg m^{-3} (VI.RUR, BL.RUR1) to 50 µg m^{-3} (VR.TRA3), while NO_2 ranged

from 4 μg m^{-3} (BL.RUR1) to 53 μg m^{-3} (VR.TRA3) and NO_x from 5 μg m^{-3} (BL.RUR1) to 130 μg m^{-3} (VR.TRA3). Comparing results averaged over 2008/14 with the annual EC limit value for NO_2 (40 μg m^{-3} averaged over one year), the limit was substantially exceeded at six traffic sites (VE.TRA2, VE.TRA1, VI.TRA, VR.TRA2, PD.TRA, VR.TRA3).

3.3. Ozone

In rural sites, average O_3 levels ranged from 48 μg m^{-3} (RO.RUR) to more than 90 μg m^{-3} (BL.RUR1, VI.RUR), while urban and suburban sites varied between ~40 and ~60 μg m^{-3}. Despite the low number of sites measuring ozone in traffic and industrial environments, it is evident that polluted environments generally exhibit the lower average concentrations: the minimum levels were recorded at VR.TRA3 (36 μg m^{-3}), which, inversely, shows the highest NO concentrations (it is located close to a large logistic intermodal freight transport hub and, thus, it is affected by heavy diesel-powered truck traffic).

Ozone is the subject of several regulations: the alert threshold (maximum 1-hour level of 240 μg m^{-3}) was never breached in 2008–2012, but was exceeded five times in 2013 at PD.RUR1. This result recalls the anomaly of PD.RUR1 already reported for PM_{10}-bound polycyclic aromatic hydrocarbons (Masiol et al., 2013). Despite PD.RUR1 being originally located far from direct emission sources, it probably suffers from a local unknown source of air pollution. In addition, it is located between and equidistant from three main urban settlements (Mestre, Padova and Treviso). Further studies should be carried out to detect the potential sources; in the meanwhile, its categorization should be revised.

The information threshold (180 μg m^{-3} over 1 h) was frequently exceeded at most of the sites. VI.RUR deserves special attention because it is affected annually by 39–126 exceedances; it is located in a remote area (1366 m asl) characterised by grass- and wood-lands and is not affected by direct anthropogenic sources. Consequently, high O_3 levels may be linked to the transport of air masses containing ozone or ozone-precursors from the nearby highly populated plain areas or to the local biogenic emission of ozone-precursors from plants. In addition, since this area is not impacted by traffic, titration of photochemically produced ozone by primary NO is negligible.

The EC long-term target value of 120 μg m^{-3} and the WHO air quality guideline of 100 μg m^{-3} measured as maximum daily 8 hour running averages (not to be exceeded more than 25 days over 3 years for the EC target) were also frequently breached at almost all the sites. Similarly, the long term objective value for the protection of vegetation (AOT40) calculated over the warm period (May to July) is also amply breached at all the rural sites, posing a serious risk to high-quality agriculture promoted by regional policies.

It is therefore evident that ozone is a critical pollutant across the Veneto. The standards for ozone are more difficult to achieve across the warmer regions (southern Europe) because of the larger magnitude of summer photochemical O_3 episodes. In addition, O_3 levels are also influenced substantially by the extent of reactions with local NO emissions, which are currently falling in Europe (Colette et al., 2011) in order to comply with the increasingly stringent emission standards required for road vehicles. As a result, recent decreases in NO emissions across Europe may limit reaction with O_3, which is the main sink of O_3 in the polluted atmosphere.

3.4. NO_x partitioning and total oxidants (OX)

Recent changes in emission trends for some air pollutants and the complex photochemistry of the NO-NO_2-O_3 system are further evaluated through two derived parameters. The partitioning of nitrogen oxides was investigated through the NO_2/NO_x ratio (Fig. 2 and Fig. SI1b) and total oxidants ($OX = NO_2 + O_3$, expressed as ppb) are often used to describe the oxidative potential (Kley et al., 1999; Clapp and Jenkin, 2001). Results are highly variable, but higher ratios are generally recorded at rural sites because of the lower primary NO emissions. The average levels of OX show little variation across the Region with distributions typically showing interquartile ranges between 25 and 50 ppbv. The highest site averages are seen at rural sites due to photochemical ozone creation, and at traffic sites, presumably caused by high emissions of primary NO_2.

3.5. Particulate matter

PM_{10} and $PM_{2.5}$ are critical air pollutants in Veneto. Average PM_{10} levels over 2008/14 varied from less than 20 μg m^{-3} in BL.RUR2 and VR.RUR to more than 40 μg m^{-3} in VI.URB1 and VI.TRA. Some sites breached the European annual Limit Value of 40 μg m^{-3} (PD.IND3, VI.URB1, PD.URB, VR.TRA2, VE.TRA1, PD.TRA and PD.IND1), except in 2013 and 2014 when no exceedances were recorded. At such sites, the annual average concentrations are usually close to the European Limit Value: consequently, small fluctuations in PM_{10} levels may have a large effect in determining them as "fulfilling" or "not fulfilling" the EC standard. However, every year more than 20 sites exceeded the daily mean of 50 μg m^{-3} for more than 35 times in a calendar year. Among these sites, VI.URB1, VE.TRA2, VE.IND and VE.URB3 showed the highest number of daily exceedances for a minimum of 77, 66, 64 and 60 times in a calendar year, respectively.

The $PM_{2.5}$ monitoring network started its operation in 2009, when the Directive 2008/50/EC entered into force, and continued to grow over the following years. Only 8 sites provide sufficient data to be included in this study. The annual limit value (25 μg m^{-3}) was frequently breached (five years out of six) at PD.URB, PD.IND1, PD.IND2, VE.IND and VI.URB1. Similar to PM_{10}, in 2013 only 6 stations breached the annual average value, while no exceedances were recorded in 2014.

4. Discussion

4.1. Differences among sites

Maps showing the average levels of recorded pollutants over the 2008/14 period are reported in Fig. SI1a,b for different site categories. Levels of CO are generally low across the region and do not show any evident trend among site categories. On the contrary, nitrogen oxides, SO_2, PM_{10} and $PM_{2.5}$ show levels increasing from rural to urban to traffic sites, while concentrations in industrial sites are highly variable and reflect the specific characteristics of each site (Fig. 2). Such patterns are opposite to ozone (higher levels at rural sites in high mountain environments and lower at sites polluted with primary emissions).

Motor vehicles are major sources of NO (Keuken et al., 2012; Kurtenbach et al., 2012) and a series of volatile organic compounds (VOCs) (Gentner et al., 2013). Munir et al. (2012) have shown that emissions from cars, buses and heavy vehicles have strong effects on urban decrements of ozone levels. Due to this, the lower O_3 levels in most anthropogenically affected sites in Veneto are related to the primary emissions of NO. This fact is further well supported by the partitioning of nitrogen oxides (Fig. SI1b): lower NO_2/NO_x ratios are recorded at urban and hot-spot sites, indicating that high relative concentrations of NO lead to ozone depletion. Another reason is linked to the impact of natural sources of VOCs, such as biogenic isoprene and terpenes, i.e. known effective ozone-precursors (Duane et al., 2002). The land cover map (Fig. 1) shows that the hilly and mountain areas of N Veneto are covered by forests. Thus, biogenic VOCs are expected to be elevated in rural and mountain environments and enhance the generation of ozone. In this context, modelling studies in Europe indicate that biogenically-driven O_3 accounts for ~5% in the Mediterranean region (Curci et al., 2009).

The Kruskal-Wallis analysis of variance by ranks (KW_{test}) was applied as a global non-parametric test for depicting statistically significant inter-site variations. The null hypothesis is rejected for $p < 0.05$, meaning that the sites in a category are statistically different. In this case, the post-hoc test after Nemenyi (Demšar, 2006) was applied for

multiple sample comparison to point out the pairs of sites which differ significantly in the pollutant level. Generally, results indicated that air pollutants are uniformly distributed across the region: no pairs of sites differ in the levels of CO, while only the two remote RUR sites (BL.RUR1 and VI.RUR) present statistically significant differences for NO_x and ozone from a large number of other sites. The application of comparison tests for PM_{10} is complicated by the lack of data at the two remote sites and by the availability of differently time resolved data (hourly and daily). Despite such limitations, results indicate that only BL.RUR2 exhibits significantly lower concentrations than other sites.

4.2. Differences among site categories

KW tests indicated that the concentrations of many pollutants measured across the Veneto are statistically similar even at sites which are categorized differently (except for the two sites located in extremely remote mountain areas). Moreover, the results point to an important conclusion: air pollutants are almost uniformly distributed across the region. However, these results also indicate that there is an apparent homogeneity among sites, i.e. sites having different categorization may experience statistically similar levels of air pollutants. This hypothesis was tested statistically using data depth (DD) analysis. However, there are some limitations to its application: the important fraction of missing data for some pollutants/sites and the lack of the full set of pollutants at most sites limits the possibilities for its use. Therefore, data-depth classifications were separately performed for: NO, NO_2 and NO_x, (ii) PM_{10}, (iii) CO. Since few TRA and IND sites measured O_3 and SO_2, the DD analysis was not possible for these pollutants because not all the site categories would be adequately represented. Application to one or a few pollutants has the disadvantage of processing pollutants separately; however, it also has the advantage that it ensures the presence of a reasonable high number of sites, which make the results more robust and the spatial extent of the analysis more extensive.

The DD classification for nitrogen oxides (Fig. 3) shows that most of RUR and URB sites are generally well separated, i.e. they are plotted far from the 1:1 bisecting line. Rural sites are also well separated from traffic and industrial ones. However, some exceptions are found. BL.SUB, VI.URB3, VI.URB4 and RO.SUB are more similar to RUR than to URB sites, i.e. NO_x levels are generally lower than other urban sites, as also confirmed by boxplots in Fig. 2. On the contrary, PD.RUR1 and RO.RUR lie on the URB-side of the DD plot, i.e. they are more comparable to URB than RUR sites. Although the anomalously high levels of air pollution at PD.RUR1 were already recognised and discussed (Masiol et al., 2013), this result also shows that two rural sites probably experience relatively high levels of NO_x with respect to remaining RUR sites.

Although levels of pollutants in sites categorized as rural generally differ from other categories, there is not a clear separation among URB, TRA and IND sites. In fact, the DD classification analysis has demonstrated that most of the TRA and IND sites can be grouped with URB sites (points lay around the bisector of the plot). DD-plots of PM_{10} also show this behaviour, while no clear classification was possible using CO (Figs. SI2 and SI3), i.e. CO levels are quite similar at all site categories.

EU directives assume that URB sites are representative of the exposure of the general population, while TRA and IND sites should be representative of areas where the highest concentrations may occur. However, results show that this condition is rarely fulfilled in Veneto. In this context, a recent position paper (JRC-AQUILA, 2013) has pointed out the need to implement criteria for improving the classification and representativeness of air quality monitoring stations in Europe. There are several reasons that may explain failure of the classification:

- The widespread distribution of emissions. Since the flat areas of the Po Valley host a 'sprinkled' continuum of urban settlements with different sizes, densities and uses (Romano and Zullo, 2015), the rather constant presence of anthropogenic emissions leads to a widespread distribution of emission sources. As a consequence, air pollutants emitted by different sources mix in the atmosphere and the limited atmospheric circulation in Po Valley further limits their dispersion.
- The similarity of URB and TRA sites probably results from urban planning. Most large cities have ancient origins and contain medieval or even Roman city centres with historic buildings and narrow streets. A rapid and intense urbanization was experienced in Italy after World War II with fast build-up of large urban/suburban areas all around the ancient city centres, often without a well-informed approach to urban planning. Consequently, some city configurations inevitability limit the movement of road traffic and are characterised by busy streets which are frequently congested during rush hour periods, i.e. when traffic is widespread over the city centres and not properly channelled into main orbital or bypass roads. The high density of emissions leads to a high level of pollution from road traffic across cities and to the consequent similar levels of pollutants between URB and TRA sites.
- The poor differentiation between URB and IND sites may result from the lack of large industrial zones (except in VE). Most of Veneto cities host small and medium-sized industries in several sectors: glass, cement, food products, wood and furniture, leather and footwear, textiles and clothing, gold jewellery, chemistry, metal-mechanics and electronics. Large industrial zones are only present in VE (Porto Marghera). In addition, during the last 20 years, a large number of companies have relocated their plants abroad, while the global financial crisis (2007/9) has overwhelmed the industrial and economic sectors with a consequent decrease in the production of goods and/or the collapse, closure or downsizing of many companies/industries. Today, small/medium sized industrial areas are scattered across the region, with many of the more significant industries located close to major cities. As a result, some IND sites can be more affected by urban sources than industrial emissions. For example, Porto Marghera, the main industrial area of Veneto, lies SE of the city of Mestre. VE.IND (representative of Porto Marghera) is located just east of the industrial area (Fig. SI4). During winter frequent temperature inversions are responsible for the build-up of air pollutants (mostly NO_x, PM) and VE.IND lies just downwind of the urban area of Mestre under prevailing wind regimes (wind rose in Fig. SI4), while it is rarely downwind of the industrial area. Consequently, in winter VE.IND is likely to be more affected by the plume from the urban area than by the industrial emissions. This hypothesis is also confirmed by previous studies (Squizzato et al., 2014; Masiol et al., 2012, 2014b), which reported similar concentrations of PM-bound species between VE.IND and the city centre of Mestre. Further modelling studies are needed to inform enhancements to the monitoring network and to better sample the industrial emissions.

4.3. Spatial gradients

The characteristics of anthropogenic pressures and the peculiar topography strongly influence the pollutant distribution: this make the quantification of pollutant gradients very challenging. RUR sites can be used as good estimators for determining gradients across the region because they can be considered as representative of the regional pollution as suggested by Lenschow et al. (2001) for PM: they are located away from large sources and are also fairly uniformly distributed across the region. Average concentrations at RUR sites have therefore been spatially interpolated to investigate the gradients of background levels of air pollutants across the region. Semi-variograms were investigated, showing that all pollutants do not all have the same direction, and ordinary kriging was selected as the best model to interpolate the data. In this study kriging analysis merely aims to shape the background gradients because it was applied over a limited number of points (9). Maps for pollutants recorded at more than six sites (NO_x, O_3, OX) are provided

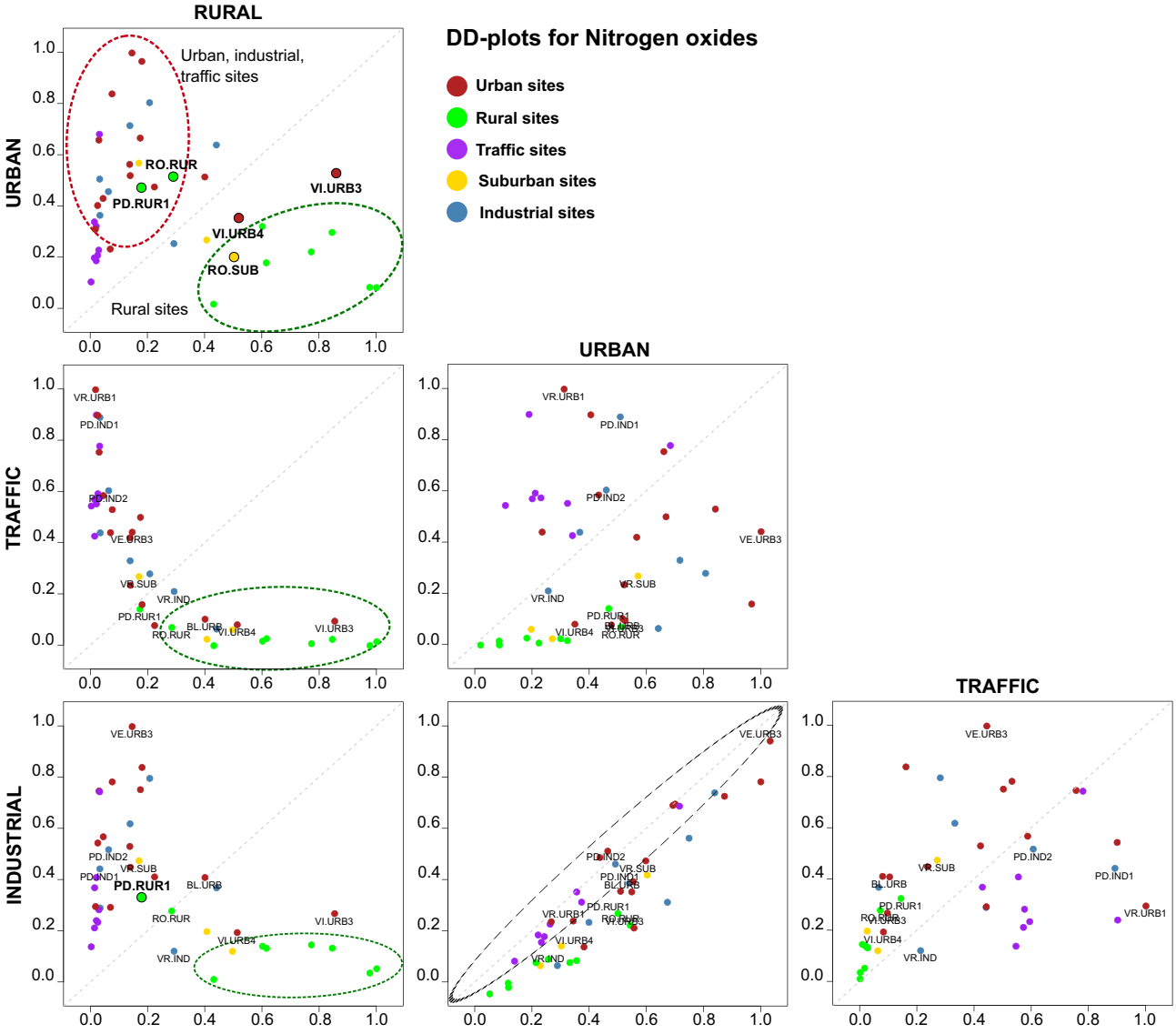

Fig. 3. Classification of the stations based DD-plot for nitrogen oxides. The analysis is based on multivariate functional simplicial data depth using nitrogen oxides (NO, NO_2 and NO_x).

in Fig. 4, while the standard errors of predictions are shown in Fig. SI5. All variables show marked gradients. Nitrogen oxides increase from the mountain environments in the north to the coastal plain areas; however the direction of maximum slopes in the increases differ slightly: NO from NW to SE, while NO_2 is from NNW to SSE. The gradient for ozone is opposite to NO, with maximum concentrations at high mountain rural sites and minima in coastal areas. The clear anti-correlation between the gradients of NO and O_3 clearly depicts their

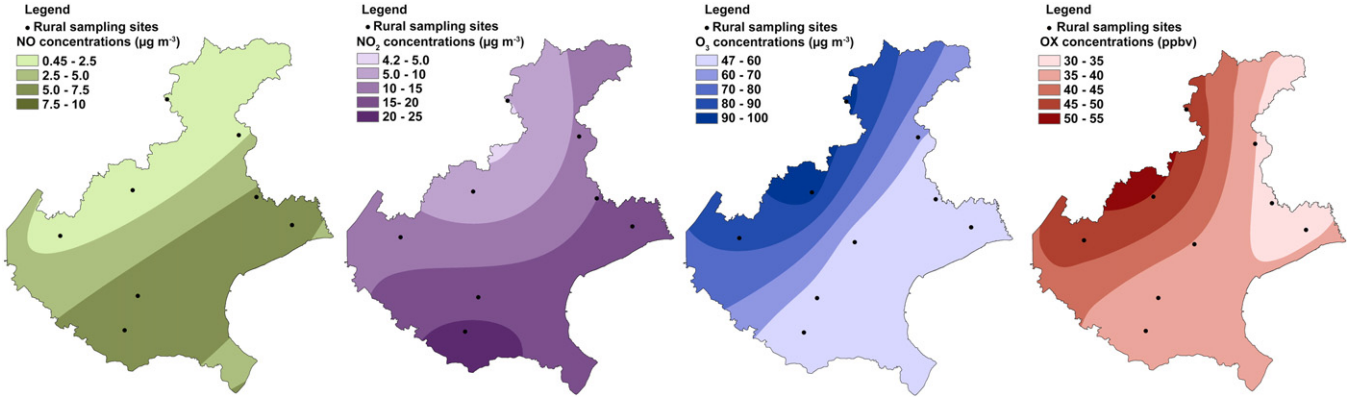

Fig. 4. Maps of concentrations for NO, NO_2, O_3 and OX measured at the RUR sites. All RUR sites were used to interpolate data for O_3 and OX, while PD-RUR1 was not used for NO and NO_2 because of the anomalously high levels recorded. Ordinary kriging method was used for interpolation. Maps showing the standard errors associated with predictions are shown as Fig. SI5.

relationship: at rural sites, NO emissions from anthropogenic sources are low and therefore, the reaction with ozone is its main sink, and the main sink for ozone. Due to the low concentrations of NO_2 at RUR sites when compared to ozone, gradients for OX are similar to those of ozone.

4.4. Seasonal patterns

The monthly-resolved distributions of air pollutants are reported in Fig. 5. No evident seasonal patterns are found for the two high-mountain sites (BL.RUR1 ad VI.RUR). At the remaining sites, all the pollutants except SO_2 exhibit clear seasonal cycles. CO, NO, NO_2, NO_x, PM_{10} and $PM_{2.5}$ show significantly higher levels in colder months (KW_{test} at $p < 0.05$). Rapid increases occur between mid-September and December; falls in concentration occur between March and mid-April. This pattern can be attributed to the interplay of some covariant causes:

- The lower mixing layer heights in winter, which limit the dispersion of pollutants emitted locally. The typical planetary boundary layer height in the Po Valley is 450 m in winter, and rises up to 1500–2000 m in the warmer months due to the thermal convective activity (Di Giuseppe et al., 2012; Bigi et al., 2012).
- Ambient temperature controls the gas-particulate phase partitioning of semivolatile compounds (ammonium nitrate and part of organic carbon). In Veneto nitrate accounts for 0.1–0.5 μg m^{-3} (0.7–2.5% of $PM_{2.5}$ mass) in August and for 5–10 μg m^{-3} (16–25%) in February (Masiol et al., 2015) and organic carbon in $PM_{2.5}$ varies from about 2.6 μg m^{-3} in June and 11.4 μg m^{-3} in December (Khan et al., 2016).
- Increased emissions in the coldest months mainly driven by increasing energy demand for domestic heating. Domestic heating is regulated at national level: generally, the switching on is fixed to occur on 15 October, while the switching off is on15 April, i.e. when the fastest changes occur. However, such dates can change according to the weather. Wood smoke from domestic heating may contribute appreciably to higher winter concentrations of PM.
- the drop of actinic fluxes in winter and the consequent reduction of hydroxyl radical, ozone, and the oxidative activity which is a sink for many pollutants.

Ozone shows a strong seasonal pattern. Ozone shows the highest values during the warmest period (generally April–September), when the solar radiation is higher (Fig. 5) and the atmospheric photochemistry is more active. Generally, ozone levels reach approx. 20 μg m^{-3} in winter, but never drop below 50 μg m^{-3} at RUR sites located in high mountain environments (BL.RUR1, VI.RUR, VR.RUR >800 m above sea level). The patterns of OX are dominated by ozone both in rural and polluted sites: the highest levels were reached in the rural mountain sites (BL.RUR1 2020 m asl; VI.RUR 1366 m asl and VR.RUR 824 m asl).

Sulphur dioxide lacks a clear seasonal pattern. Industrial emissions are expected to be quite constant through the year, but highest emissions of SO_2 are may occur in summer due to an increase in energy production from coal power plants to meet air conditioning demand. However, the higher mixing layer height and the enhanced photochemistry driving S(IV) to S(VI) conversion lead to similar concentrations to the cold period.

4.5. Daily and weekly patterns

Fig. 6 reports the diurnal cycles, while Fig. SI6 shows the weekly patterns. As for the seasonal patterns, daily cycles are the result of interplays among the strength of sources, photochemical processes and weather factors. Although minor changes due to peculiar local conditions are found, almost all the sites exhibit rather similar daily and weekly cycles, except at the three high mountain sites. CO and nitrogen oxides show typical daily cycles linked to road traffic at almost all the sites, with two daily peaks corresponding to the morning and evening rush hours (7–9 am and 6–8 pm). The morning and evening peaks are split by a minimum, which is assumed to be the result of: (i) lower emissions (less traffic); (ii) larger availability of ozone driven by the daylight photolysis of NO_x and the oxidation of VOC and CO (iii) higher convective activity leading to a deeper mixed layer, which enhances the atmospheric mixing. Weekly patterns are also linked to road traffic: generally, average levels increase from Mondays to Thursdays, while a fast drop is measured during weekends, when road traffic reach minimum volumes and heavy duty vehicles over 7.5 tonnes are subject to some limitations (over the whole weekends in summer and on Sundays in winter).

Ozone and total oxidants (OX) show evident daily peaks in the mid-afternoon, i.e. the hours experiencing the higher solar irradiation, and lower levels are experienced between 6 and 9 am local time (DST time-corrected in summer). These patterns are also enhanced in summer due to the higher solar irradiation. It is evident that daily peaks of OX are delayed 2–3 h with respect to ozone, corresponding to the increased NO to NO_2 oxidation and primary NO_2 emissions in evening rush hours. The weekly patterns are the mirror images of CO and NO_x with higher concentrations during the weekends, following the drop of fresh anthropogenic emissions. However, such marked diurnal patterns are not found at the three high mountain sites, which show rather constant and high levels throughout the day. This "flatter" pattern has also been observed at other high-mountain sites in the Apennines (Cristofanelli et al., 2007) and Alps (Vecchi and Valli, 1998) and is likely related to the lack of anthropogenic sources of freshly emitted ozone-precursors and the presence of higher levels of biogenic ozone-precursors, which do not follow anthropogenic cycling. However, the levels of ozone in high mountain environments are also known to be strongly affected by (i) the transport of polluted air masses by local wind systems (valley and slope winds) from the Po Valley and surrounding cities inside the Alps (Kaiser, 2009), Foehn wind events (Seibert et al., 2009), large scale synoptic air pollutant transport (Wotawa et al., 2000) and stratospheric inputs (Vingarzan, 2004). Nocturnal dry deposition is also less effective at mountain sites.

Daily cycles of SO_2 are quite different thorough the region and between site categories and show two different patterns. Most sites present NO_x-like patterns, i.e. two weak peaks corresponding to the morning and evening rush hours. On the contrary, all RUR sites plus all sites in VE (with different categorizations) and VI-URB3 (190 m asl) exhibited diurnal patterns very similar to ozone, i.e. higher levels in the middle of the day. The two patterns remain different throughout the year: different source emissions and weather factors may explain such patterns. The first cycle is related to road traffic and is more evident at VR-TRA3 (close to a large logistic intermodal freight transport hub), where the highest levels of NO_x are recorded. In Europe, sulphur content in automotive gasoline and diesel is now limited to <10 ppm (since 2009), however it is clear that large volumes in traffic and congestion during rush hours may have a key effect in shaping the diurnal SO_2 levels. The second pattern was previously seen in Venice-Mestre (Masiol et al., 2014c) and was related to local emissions from the nearby industrial zone hosting a large coal-fired power plant and a large oil refinery, which are well known strong sources of SO_2, as indicated by local emission inventories (ISPRA, 2015; ARPAV – Regione Veneto, 2015). The closeness of VE sites to the sea drives the presence of sea/land breezes (mainly in warmest periods) and has a strong influence of the local circulation pattern and in bringing air masses from the industrial zone to the site locations. The daytime increase in SO_2 was also reported for a background site in London by Bigi and Harrison (2010) who attributed it to the downward mixing of plumes from elevated point sources as the boundary layer deepens during daylight hours.

Generally, PM_{10} exhibits higher concentrations overnight and clear minima in the early afternoon. This pattern is consistent with the diurnal dynamics of the mixing layer. However, a secondary cause may be related to the volatilisation of the more volatile aerosol compounds

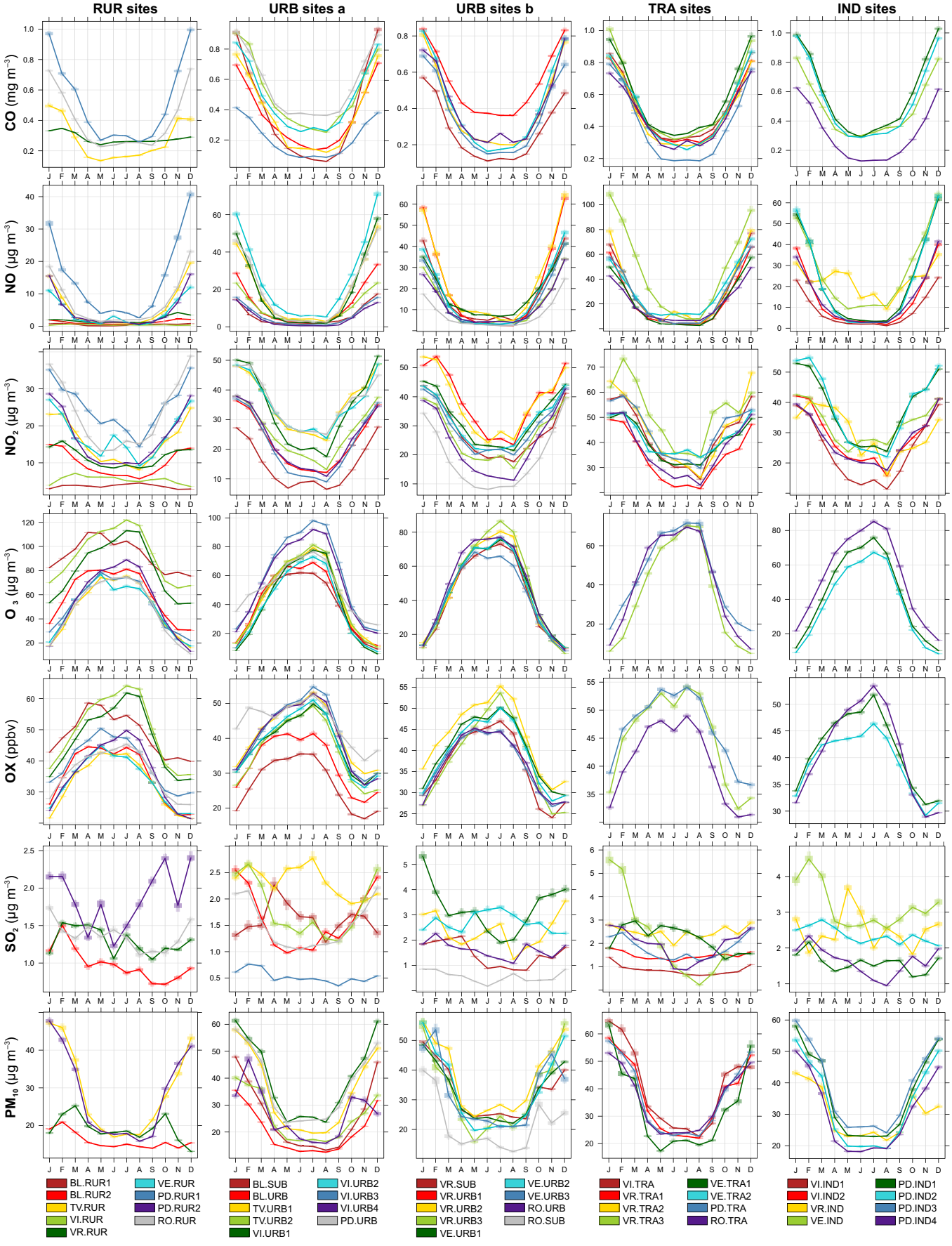

Fig. 5. Seasonal variations of the monitored pollutants. Each plot reports the monthly average levels as a filled line and the associated 75th and 99th confidence intervals calculated by bootstrapping the data (n = 200).

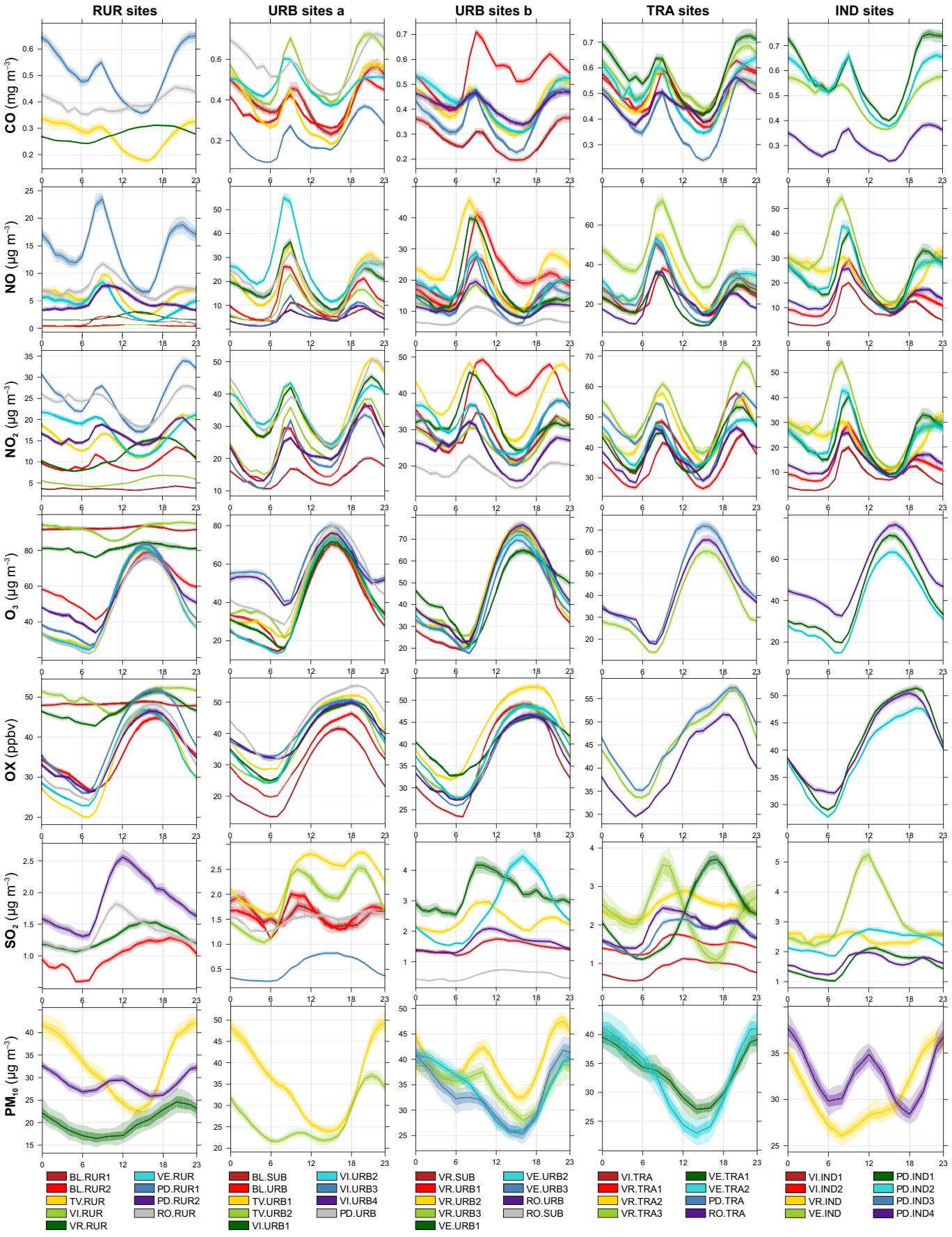

Fig. 6. Diurnal variations of levels of measured pollutants computed over the hourly averaged data during the sampling period. Each plot reports the average level as a filled line and the associated 75th and 99th confidence intervals calculated by bootstrapping the data (n = 200). Data are corrected for DST.

(e.g., nitrate) during the early afternoon, i.e. when the air temperature is higher and relative humidity lower. Minor peaks of PM_{10} concentrations can be found just before noon at a few sites affecting by very different emission scenarios (VR.URB2, VR.URB3, VE.URB3, PD.RUR2, PD.IND4). Their interpretation is not clear and may be related to the local characteristics of the sites.

4.6. Long-term trends

The long-term trends were analysed using the monthly-averaged data: since missing data can significantly affect the trend analysis, only months having at least 75% of available records were processed. In addition, only trends over periods extending more than 4 consecutive years were computed. The quantification and the significance of the trends were evaluated by applying the Theil-Sen nonparametric estimator of slope (Sen, 1968; Theil, 1992). This technique assumes linear trends and is therefore useful to estimate the interannual trends, but it is irrespective of the shape of trends. The slopes were also deseasonalized by using the seasonal trend decomposition using loess (STL) to exclude the effect of the seasonal cycles. Details of STL are provided in Cleveland et al. (1990). The statistics of the linear trends are listed in Table SI1 as percentage y^{-1}, while Fig. SI7 shows all the single trends expressed in concentration y^{-1} along with the upper and lower 95th confidence intervals in the trends and the *p*-values, which indicate the statistical significance of the slope estimation.

The trends observed at each site reflect both regional and local changes and are affected by the particular characteristics of the site locations. However, when trends observed at individual sites are aggregated at provincial or regional levels, their relationships with current and past emissions inventories can be examined. The slopes calculated with the Theil-Sen method are then compared with changes in primary emissions as reported in various emission inventories (EIs) available at both regional and provincial level.

For each pollutant, statistically significant ($p < 0.05$) trends expressed in percentage y^{-1} are provided in Fig. 7 along with: (i) the differences in estimated emissions between 2010 and 2005 at provincial level provided by the EI SINAnet top-down (ISPRA, 2015) and (ii) the differences between 2010 and 2007/8 at regional scale provided by

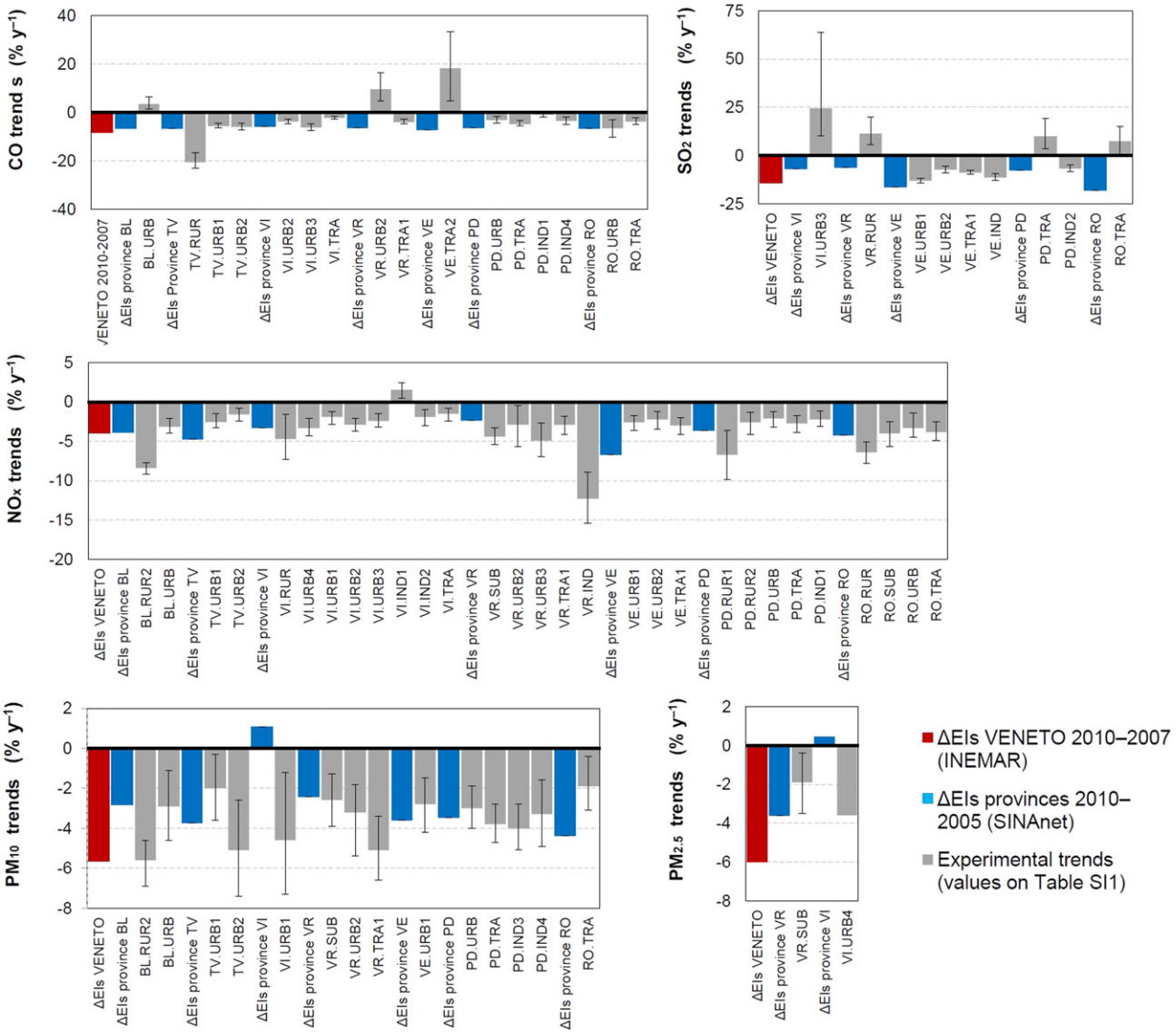

Fig. 7. Results of the Theil-Sen analysis of trends (grey bars). The estimated trends are expressed as percentage; the confidence intervals of trends are given by error bars. Only sites showing significant trends (*p*-values < 0.05) are shown. The percentages of change in emissions provided by the most recent emission inventories are also provided and expressed as % y^{-1}: changes of EIs for the whole Veneto region (Δ_Veneto, red bars) refers to the difference of EIs between 2010 and 2007; changes of EIs for each province (Δ_BL, Δ_TV, Δ_VI, Δ_VR, Δ_VE, Δ_PD, Δ_RO, blue bars) refers to the difference of EIs between 2010 and 2005.

INEMAR (ARPAV – Regione Veneto, 2015). Differences of EIs (ΔEIs) are also expressed as percentage y^{-1} for an easier comparison with measured data (this choice considers a linear trend throughout the considered periods). Generally, most of the trends are negative for all the species and the changes in measured concentrations of CO, NO_x, PM_{10}, $PM_{2.5}$ agree well with EIs. However, some exceptions are also found (note that not all sites revealed statistically significant slopes).

CO concentrations decreased significantly at 12 of 18 sites with more than four years of available data, with slopes between −20.5% y^{-1} (TV.RUR) and −1% y^{-1} (PD.IND1). This result is in line with the average drops by −6.5% reported by INEMAR for the whole Veneto and with the EIs provided by SINAnet at province scale. However, some sites show the opposite behaviour, i.e. increased concentrations: BL.URB (+3.5% y^{-1}), VR.URB2 (+9.6% y^{-1}) and VE.TRA2 (+18.2% y^{-1}). Since falls of CO in EIs are mainly driven by road transport and non-industrial combustion (including biomass burning), such sites have possibly experienced local increases of road traffic volumes or emissions from the use of wood for domestic heating, which is widely used in mountain areas (mainly BL).

The average decrease of NO_x levels across the whole region was estimated as −4.1% y^{-1} by INEMAR and was mainly attributed to "road transport" and, secondarily, to "combustion in energy and transformation industry" and "combustion in industry" sectors. The average slope from data measured experimentally at all the sites was −3.5% y^{-1}, ranging between −12.3% y^{-1} (VR.IND) and −1.5% y^{-1} (VI.TRA). Statistically significant trends were negative at all sites except at VI.IND (+1.5% y^{-1}). This result is a positive finding meaning that abatement strategies and improvement of technologies had an effect in reducing the ambient levels of NO_x. However, in recent years there has been increasing interest in NO_x emissions and NO/NO_2 partitioning in Europe. Evident discrepancies have been found between achieving NO_x emission reductions and NO_2 ambient concentrations, which do not meet the targets in many locations (e.g., Grice et al., 2009; Cyrys et al., 2012). These concerns have been related to the recent increase in NO_2 levels in Europe due to the increased proportion of diesel-powered vehicles, which are known to have higher primary (direct) emissions of NO_2 (Carslaw et al., 2007; Anttila et al., 2011). Since the recent boom of diesel vehicles was also experienced in Italy (Cames and Helmers, 2013), the relationship between significant trends of NO_x and NO_2 needs to be further investigated.

Analysis of trends in SO_2 requires particular care. Based on EIs estimations, a significant drop (−14% y^{-1}) was experienced across the whole region, while at province level SO_2 emissions decreased between −18% y^{-1} (in RO) and −6% y^{-1} (in BL). These drops in EIs are principally attributed to the sector of combustion in energy transformation industries. In Veneto, this sector is mostly represented by the energy production in coal-fired power stations, which is present in VE province (Porto Marghera). In addition, the sector of 'other mobile sources' has also experienced significant drops, particularly of ship emissions (present only in coastal areas of VE province): from January 2010, ships in the harbours are requested to use fuels with sulphur content <0.1%. According to the EIs, experimental data show that all sites in the VE province and PD.IND2 have negative trends, while four sites have experienced statistically significant increases in SO_2 levels, i.e. VI.URB3 (+24.5% y^{-1}), VR.RUR (+11.4% y^{-1}), PD.TRA (+9.9% y^{-1}) and RO.TRA (+7.4% y^{-1}). While the decline at VE sites may be attributed to the concurrent fall in industrial and maritime source emissions at a local scale, the increases at other sites deserve further investigation and are possibly due to long-range transport of polluted air masses. In this context, a recent study (Masiol et al., 2015) has reported that Eastern Europe is a potential source area for $PM_{2.5}$-bound sulphate, i.e. the major sink for atmospheric SO_2.

Measured data fit well with changes in EIs for PM_{10}, except in VI province. All statistically significant trends calculated from field data show decreases in PM_{10} concentration ranging between −5.6% y^{-1} in BL.RUR2 and −1.9% y^{-1} in RO.TRA. PM_{10} emissions estimated by EIs dropped between −4.4% y^{-1} in RO province and −2.4% y^{-1} in VR, with a slight increase in VI (+1.1% y^{-1}). At a regional scale, the INEMAR inventory reports an overall decrease of −5.7% y^{-1}. Results for $PM_{2.5}$ are quite variable, mostly due to the short series of available experimental data: only 3 sites present more than 4 years of data, of which only 2 have statistically significant trends. Hence, no further information can be extracted for $PM_{2.5}$.

5. Conclusions

Air quality data from 43 monitoring sites have been used as input for a number of statistical tools to assess the extent of air pollution across the Veneto. This paper is the first one providing information from a large number of sites over a wide region of N Italy. The main findings can be summarised as follows:

- Carbon monoxide and sulphur dioxide show low levels across the region and, therefore, are not considered as critical pollutants. While CO does not show any evident spatial trend, SO_2 levels are higher in VE Province, particularly around Venice-Mestre. This anomaly was linked to the industrial zone (coal power plant, oil refineries, other industrial installations) and harbour activities;
- Nitrogen dioxide, ozone and particulate matter (both PM_{10} and $PM_{2.5}$) are critical pollutants in view of protecting human health, i.e. the EC limit and target values are frequently breached at some sites. Those air pollutants deserve special attention because of their known adverse effects upon public health: future mitigation strategies should focus on reducing concentrations of such key pollutants;
- Air pollutants are quite uniformly distributed across the region: no pairs of sites have statistically significant differences in the levels of CO, while only the two remote rural sites present statistically significant differences from a large number of other sites for NO_x and ozone;
- The current site categorization was tested by applying a data depth classification analysis: results show that sites categorized as rural generally differ from other categories, while there is not a clear separation among urban background, traffic and industrial sites. Probable causes of the poor classification are discussed; some insights for improving the monitoring network are provided;
- Spatial trends were investigated by interpolating average concentrations at the rural sites: despite NO and NO_2 having a slightly different direction of maximum slopes, nitrogen oxides generally increase from the mountain to the coastal plain environments, while ozone presents maxima concentrations at high mountain rural sites and minima in coastal areas;
- Seasonal pattern analysis revealed that CO, NO, NO_2, NO_x, PM_{10} and $PM_{2.5}$ show significantly higher levels in colder months and minima in summer. This pattern is mainly attributed to the lower mixing layer heights, the limited oxidation potential and the emissions from domestic heating. The volatilization of semi-volatile aerosol compounds during the warmer seasons is another reason of this behaviour for PM. On the contrary, ozone has an opposite seasonality with maxima in summer due to its increased photochemical generation. No seasonal patterns are found for SO_2;
- Diurnal and weekly cycles were investigated. Generally, similar patterns are observed across the region for all the measured species. A strong potential effect of road traffic emissions was found for CO and nitrogen oxides: one/two daily peaks are commonly found at urban and hotspot sites and were related road traffic emissions during rush hours. Ozone cycles were shaped by the photochemistry and by the interplay with NO. PM cycles generally show higher levels overnight and, therefore, are mostly shaped by the mixing layer height dynamics;
- An overall decrease of all measured species (except ozone) was observed throughout the region. Generally, results of trend analysis well fit with changes in emission inventories. However, some sites with opposite trends have been identified; the reasons for increasing concentrations in such sites needs to be further investigated.

Disclaimer

The views and conclusions expressed in this paper are exclusively of the authors and may not reflect those of ARPAV.

Acknowledgements

We gratefully acknowledge: (i) ARPAV for providing data; (ii) the European Environment Agency for providing CORINE Land Cover 2006 data.

Appendix A. Supplementary data

Supplementary data to this article can be found online at http://dx.doi.org/10.1016/j.scitotenv.2016.10.042.

References

Agostinelli, C., Romanazzi, M., 2011. Local depth. J. Stat. Plan. Inference 141 (2), 817–830.

Agostinelli, C., Romanazzi, M., 2013. Nonparametric analysis of directional data based on data depth. Environ. Ecol. Stat. 20 (2), 253–270.

Anttila, P., Tuovinen, J.P., Niemi, J.V., 2011. Primary NO_2 emissions and their role in the development of NO2 concentrations in a traffic environment. Atmos. Environ. 45 (4), 986–992.

ARPAV (Environmental Protection Agency of Veneto Region), 2011. Relazione Regionale Qualità dell'aria – Anno. ([in Italian], 2012. Available from: http://www.arpa.veneto.it/temi-ambientali/aria/riferimenti/documenti/documenti-1 (last accessed: June 2015)).

ARPAV (Environmental Protection Agency of Veneto Region), 2014. Relazione Regionale Qualità dell'aria – Anno 2013. ([in Italian]. Available from: http://www.arpa.veneto.it/temi-ambientali/aria/riferimenti/documenti/documenti-1 (last accessed: June 2015)).

ARPAV (Environmental Protection Agency of Veneto Region) – Regione Veneto, 2015R. INEMAR VENETO 2010 – Inventario Regionale delle Emissioni in Atmosfera in Regione Veneto, edizione 2010 – Risultati dell'edizione 2010 in versione definitiva – Relazione generale. ARPA Veneto – Osservatorio Regionale Aria, Regione del Veneto – Dipartimento Ambiente, Sezione Tutela Ambiente, Settore Tutela Atmosfera. ([in Italian]. Available at: http://www.arpa.veneto.it/temi-ambientali/aria/emissioni-di-inquinanti/inventario-emissioni [last accessed on Nov 2015]).

Bigi, A., Harrison, R.M., 2010. Analysis of the air pollution climate at a central urban background site. Atmos. Environ. 44, 2004–2012.

Bigi, A., Ghermandi, G., Harrison, R.M., 2012. Analysis of the air pollution climate at a background site in the Po valley. J. Environ. Monit. 14, 552–563.

Cames, M., Helmers, E., 2013. Critical evaluation of the European diesel car boom—global comparison, environmental effects and various national strategies. Environ. Sci. Eur. 25 (1), 1.

Carslaw, D.C., 2015. The openair manual — open-source tools for analysing air pollution data. Manual for Version 28th January 2015. King's College London.

Carslaw, D.C., Ropkins, K., 2012. Openair – an R package for air quality data analysis. Environ. Model. Softw. 27–28, 52–61.

Carslaw, D.C., Beevers, S.D., Bell, M.C., 2007. Risks of exceeding the hourly EU limit value for nitrogen dioxide resulting from increased road transport emissions of primary nitrogen dioxide. Atmos. Environ. 41, 2073–2082.

Claeskens, G., Hubert, M., Slaets, L., Vakili, K., 2014. Multivariate functional halfspace depth. J. Am. Stat. Assoc. 109 (505), 411–423.

Clapp, L.J., Jenkin, M.E., 2001. Analysis of the relationship between ambient levels of O_3, NO_2 and NO as a function of NO_x in the UK. Atmos. Environ. 35, 6391–6405.

Cleveland, R.B., Cleveland, W.S., McRae, J.E., Terpenning, I., 1990. STL: a seasonal-trend decomposition procedure based on loess. J. Off. Stat. 6 (1), 3–73.

Colette, A., Granier, C., Hodnebrog, Ø., Jakobs, H., Maurizi, A., Nyiri, A., et al., 2011. Air quality trends in Europe over the past decade: a first multi-model assessment. Atmos. Chem. Phys. 11 (22), 11657–11678.

Contini, D., Gambaro, A., Donateo, A., Cescon, P., Cesari, D., Merico, E., Citron, M., 2015. Inter-annual trend of the primary contribution of ship emissions to $PM_{2.5}$ concentrations in Venice (Italy): efficiency of emissions mitigation strategies. Atmos. Environ. 102, 183–190.

Cristofanelli, P., Bonasoni, P., Carboni, G., Calzolari, F., Casarola, L., Sajani, S.Z., Santaguida, R., 2007. Anomalous high ozone concentrations recorded at a high mountain station in Italy in summer 2003. Atmos. Environ. 41 (7), 1383–1394.

Cuevas, A., 2014. A partial overview of the theory of statistics with functional data. J. Stat. Plan. Inference 147, 1–23.

Curci, G., Beekmann, M., Vautard, R., Smiatek, G., Steinbrecher, R., Theloke, J., Friedrich, R., 2009. Modelling study of the impact of isoprene and terpene biogenic emissions on European ozone levels. Atmos. Environ. 43 (7), 1444–1455.

Cyrys, J., Eeftens, M., Heinrich, J., Ampe, C., Armengaud, A., Beelen, R., et al., 2012. Variation of NO_2 and NO_x concentrations between and within 36 European study areas: results from the ESCAPE study. Atmos. Environ. 62, 374–390.

Demšar, J., 2006. Statistical comparisons of classifiers over multiple data sets. J. Mach. Learn. Res. 7, 1–30.

Di Giuseppe, F., Riccio, A., Caporaso, L., Bonafe, G., Gobbi, G.P., Angelini, F., 2012. Automatic detection of atmospheric boundary layer height using ceilometers backscatter data assisted by a boundary layer model. Q. J. R. Meteorol. Soc. 138, 649–663.

Duane, M., Poma, B., Rembges, D., Astorga, C., Larsen, B.R., 2002. Isoprene and its degradation products as strong ozone precursors in Insubria, Northern Italy. Atmos. Environ. 36 (24), 3867–3879.

EEA (European Environment Agency), 2016. AirBased The European Air Quality Database. http://www.eea.europa.eu/themes/air/air-quality/map/airbase (accessed February 2016).

Gentner, D.R., Worton, D.R., Isaacman, G., Davis, L.C., Dallmann, T.R., Wood, E.C., et al., 2013. Chemical composition of gas-phase organic carbon emissions from motor vehicles and implications for ozone production. Environ. Sci. Technol. 47 (20), 11837–11848.

Grice, S., Stedman, J., Kent, A., Hobson, M., Norris, J., Abbott, J., Cooke, S., 2009. Recent trends and projections of primary NO_2 emissions in Europe. Atmos. Environ. 43, 2154–2167.

ISPRA, Italian Institute for Environmental Protection and Research. Disaggregated Emission Inventory. http://www.sinanet.isprambiente.it/it/inventaria/disaggregazione-dellinventario-nazionale-2010, 2015 (accessed 30 October 2015).

JRC-AQUILA, 2013. Position Paper - Assessment on Siting Criteria, Classification and Representativeness of Air Quality Monitoring Stations. (Available at: http://ec.europa.eu/environment/air/pdf/SCREAM%20final.pdf last accessed: April 2016).

Kaiser, A., 2009. Origin of polluted air masses in the Alps. An overview and first results for MONARPOP. Environ. Pollut. 157 (12), 3232–3237.

Keuken, M.P., Roemer, M.G.M., Zandveld, P., Verbeek, R.P., Velders, G.J.M., 2012. Trends in primary NO_2 and exhaust PM emissions from road traffic for the period 2000–2020 and implications for air quality and health in the Netherlands. Atmos. Environ. 54, 313–319.

Khan, M.B., Masiol, M., Formenton, G., Di Gilio, A., de Gennaro, G., Agostinelli, C., Pavoni, B., 2016. Carbonaceous $PM_{2.5}$ and secondary organic aerosol across the Veneto region (NE Italy). Sci. Total Environ. 542, 172–181.

Kley, D., Kleinmann, M., Sanderman, H., Krupa, S., 1999. Photochemical oxidants: state of the science. Environ. Pollut. 100, 19–42.

Kurtenbach, R., Kleffmann, J., Niedojadlo, A., Wiesen, P., 2012. Primary NO_2 emissions and their impact on air quality in traffic environments in Germany. Environ. Sci. Eur. 24 (12), 1–8.

Lenschow, P., Abraham, H.-J., Kutzner, K., Lutz, M., Preuß, J.-D., Reichenbacher, W., 2001. Some ideas about the sources of PM_{10}. Atmos. Environ. 35, S23–S33.

Li, J., Cuesta-Albertos, J.A., Liu, R.Y., 2012. DD-classifier: nonparametric classification procedures based on DD-plot. J. Am. Stat. Assoc. 107, 737–753.

Liu, R.Y., 1990. On a notion of data depth based on random simplices. Ann. Stat. 18 (1), 405–414.

Lopez-Pintado, S., Romo, J., 2009. On the concept of depth for functional data. J. Am. Stat. Assoc. 104 (486), 718–734.

Lopez-Pintado, S., Romo, J., 2011. A half-region depth for functional data. Comput. Stat. Data Anal. 55 (4), 1679–1695.

Masiol, M., Centanni, E., Squizzato, S., Hofer, A., Pecorari, E., Rampazzo, G., Pavoni, B., 2012. GC–MS analyses and chemometric processing to discriminate the local and long-distance sources of PAHs associated to atmospheric $PM_{2.5}$. Environ. Sci. Pollut. Res. 19 (8), 3142–3151.

Masiol, M., Formenton, G., Pasqualetto, A., Pavoni, B., 2013. Seasonal trends and spatial variations of PM_{10}-bounded polycyclic aromatic hydrocarbons in Veneto region, Northeast Italy. Atmos. Environ. 79, 811–821.

Masiol, M., Formenton, G., Giraldo, G., Pasqualetto, A., Tieppo, P., Pavoni, B., 2014a. The dark side of the tradition: the polluting effect of Epiphany folk fires in the eastern Po Valley (Italy). Sci. Total Environ. 473–474, 549–564.

Masiol, M., Squizzato, S., Rampazzo, G., Pavoni, B., 2014b. Source apportionment of $PM_{2.5}$ at multiple sites in Venice (Italy): spatial variability and the role of weather. Atmos. Environ. 98, 78–88.

Masiol, M., Agostinelli, C., Formenton, G., Tarabotti, E., Pavoni, B., 2014c. Thirteen years of air pollution hourly monitoring in a large city: potential sources, trends, cycles and effects of car-free days. Sci. Total Environ. 494–495, 84–96.

Masiol, M., Benetello, F., Harrison, R.M., Formenton, G., De Gasperi, F., Pavoni, B., 2015. Spatial, seasonal trends and transboundary transport of $PM_{2.5}$ inorganic ions in the Veneto region (northeastern Italy). Atmos. Environ. 117, 19–31.

Mosler K, Polyakova Y. General Notions of Depth for Functional Data. arXiv 2012; (arXiv: 1208.1981).

Munir, S., Chen, H., Ropkins, K., 2012. Modelling the impact of road traffic on ground level ozone concentration using a quantile regression approach. Atmos. Environ. 60, 283–291.

Pohlert, T., 2015. PMCMR: Calculate Pairwise Multiple Comparisons of Mean Rank Sums. R Package Version 1.3. http://CRAN.R-project.org/package=PMCMR.

Putaud, J.P., Raes, F., van Dingenen, R., Brüggemann, E., Facchini, M.C., Decesari, S., et al., 2004. A European aerosol phenomenology – 2: chemical characteristics of particulate matter at kerbside, urban, rural and background sites in Europe. Atmos. Environ. 38, 2579–2595.

Putaud, J.P., Van Dingenen, R., Alastuey, A., Bauer, H., Birmili, W., Cyrys, J., et al., 2010. A European aerosol phenomenology – 3: physical and chemical characteristics of particulate matter from 60 rural, urban, and kerbside sites across Europe. Atmos. Environ. 44, 1308–1320.

R Core Team. R: a Language and Environment for Statistical Computing. R Foundation for Statistical Computing, Vienna, Austria, 2016. URL https://www.R-project.org/.

Ramsay, J.O., Silverman, B.W., 2006. Functional Data Analysis. Springer.

Romano, B., Zullo, F., 2015. Half a century of urbanization in southern European lowlands: a study on the Po Valley (northern Italy). Urban Res. Pract. 8, 1–22.

Seibert, P., Feldmann, H., Neininger, B., Bäumle, M., Trickl, T., 2009. South foehn and ozone in the Eastern Alps–case study and climatological aspects. Atmos. Environ. 34 (9), 1379–1394.
Sen, P.K., 1968. Estimates of the regression coefficient based on Kendall's tau. J. Am. Stat. Assoc. 63, 1379–1389.
Squizzato, S., Masiol, M., Visin, F., Canal, A., Rampazzo, G., Pavoni, B., 2014. The $PM_{2.5}$ chemical composition in an industrial zone included in a large urban settlement: main sources and local background. Environ. Sci. Process. Impacts 16, 1913–1922.
Theil, H., 1992. A rank-invariant method of linear and polynomial regression analysis. Henri Theil's Contributions to Economics and Econometrics. Springer, Netherlands, pp. 345–381.
Vecchi, R., Valli, G., 1998. Ozone assessment in the southern part of the Alps. Atmos. Environ. 33 (1), 97–109.
Vingarzan, R., 2004. A review of surface ozone background levels and trends. Atmos. Environ. 38, 3431–3442.
WHO (World Health Organization), 2000. Air Quality Guidelines for Europe. European Series No 91, World Health Organization. WHO Regional Publications, Geneva.
Wotawa, G., Kröger, H., Stohl, A., 2000. Transport of ozone towards the Alps–results from trajectory analyses and photochemical model studies. Atmos. Environ. 34 (9), 1367–1377.
Zhu, T., Melamed, M., Parrish, D., Gauss, M., Klenner, L.G., Lawrence, M., Konare, A., Liousse, C., 2012. Impacts of Megacities on Air Pollution and Climate. WMO, Geneva.
Zuo, Y., Serfling, R.J., 2000. General notions of statistical depth function. Ann. Stat. 28 (2), 461–482.